



# Enhancement effect on antibacterial property of gray titania coating by plasma-sprayed hydroxyapatite-amino acid complexes during irradiation with visible light



Sarita Morakul<sup>a</sup>, Yuichi Otsuka<sup>b,\*</sup>, Kiyoshi Ohnuma<sup>c</sup>, Motohiro Tagaya<sup>d</sup>, Satoshi Motozuka<sup>e</sup>, Yukio Miyashita<sup>f</sup>, Yoshiharu Mutoh<sup>b</sup>

<sup>a</sup> Graduate School of Materials Science, Nagaoka University of Technology, 1603-1 Kamitomioka, Nagaoka-shi, Niigata 940-2188, Japan

<sup>b</sup> Department of System Safety, Nagaoka University of Technology, 1603-1 Kamitomioka, Nagaoka-shi, Niigata 940-2188, Japan

<sup>c</sup> Department of Bioengineering, Nagaoka University of Technology, 1603-1 Kamitomioka, Nagaoka-shi, Niigata 940-2188, Japan

<sup>d</sup> Department of Materials Science, Nagaoka University of Technology, 1603-1 Kamitomioka, Nagaoka-shi, Niigata 940-2188, Japan

<sup>e</sup> Department of Mechanical Engineering, Gifu National College of Technology, 2236-2 Kamimakuwa, Motosu, Gifu, Japan

<sup>f</sup> Department of Mechanical Engineering, Nagaoka University of Technology, 1603-1 Kamitomioka, Nagaoka-shi, Niigata 940-2188, Japan

## ARTICLE INFO

### Keywords:

Materials science  
Biomedical engineering  
Gray titania  
Antibacterial property  
HAp-amino acid fluorescent complex  
Surface potential  
TiO<sub>2</sub>  
Kelvin probe force microscopy  
Photocatalysis  
Biomechanical engineering  
Surface coating  
Surface property  
Biomaterials  
Medical implant  
Antimicrobial agent  
Materials characterization  
Electrical property

## ABSTRACT

The aim of this study was to reveal the mechanism of enhancement of antibacterial properties of gray titania by plasma-sprayed hydroxyapatite (HAp)-amino acid fluorescent complexes under irradiation with visible light. Although visible-light-sensitive photocatalysts are applied safely to oral cavities, their efficacy is not high because of the low energy of irradiating light. This study proposed a composite coating containing HAp and gray titania. HAp itself functioned as bacteria catchers and gray titania released antibacterial radicals by visible-light irradiation. HAp-amino acid fluorescent complexes were formed on the surface of the composite coating in order to increase light intensity to gray titania by fluorescence, based on an idea bioinspired by deep-sea fluorescent coral reefs. A cytotoxicity assay on murine osteoblastlike cells revealed that biocompatibility of the HAp-amino acid fluorescent complexes was identical with the that of HAp. Antibacterial assays involving *Escherichia coli* showed that the three types of HAp-amino acid fluorescent complexes and irradiation with three types of light-emitting diodes (blue, green, and red) significantly decreased colony-forming units. Furthermore, kelvin probe force microscopy revealed that the HAp-amino acid fluorescent complexes preserved the surface potentials even after irradiation with visible light, whereas those of HAp were significantly decreased by the irradiation. Such a preservative effect of the HAp-amino acid fluorescent complexes maintained the bacterial-adhesion performance of HAp and consequently enhanced the antibacterial action of gray titania.

## 1. Introduction

A titanium alloy coated with plasma-sprayed hydroxyapatite (HAp) has been widely applied to biomedical components, such as dental implants, artificial hip joints, and knee joints [1]. One of the major causes of revision of such implants is loosening [2]. The HAp coating promotes a stronger bond between surfaces of implants and human bone, thereby resulting in earlier fixation of the implants and their long service life [3, 4, 5, 6]. Nonetheless, another cause of revision procedures—bacterial infection—recently came up as a serious problem [7, 8, 9, 10, 11, 12]. Bacterial infection on the surface of implants forms a biofilm,

which causes peri-implantitis and inflammation of the surrounding tissues [12]. Damage by bacterial infection occurs in approximately 5% of cases of revision or reconstruction of orthopedic implants [7]. To prevent a fracture caused by bacterial infection, an antibacterial technology is necessary.

Two types of coating, i.e., passive coating and active coating, have been widely studied as an antibacterial agent on the surface of implants [13, 14, 15]. Passive coating is intended to prevent adhesion of bacteria to the surface of implants by controlling surface morphology, wettability, conductivity, surface charge, or crystal structure of a substrate [15, 16, 17]. Surface morphology, such as roughness or height, greatly

\* Corresponding author.

E-mail address: [otsuka@vos.nagaokaut.ac.jp](mailto:otsuka@vos.nagaokaut.ac.jp) (Y. Otsuka).

<https://doi.org/10.1016/j.heliyon.2019.e02207>

Received 29 April 2019; Received in revised form 7 June 2019; Accepted 30 July 2019

affects bacterial adhesion behavior [18, 19, 20]. Although a polished surface can reduce bacterial adhesion, such a reductive effect of the roughness decrease reaches a plateau below a certain level of roughness. Hydrophilicity of the surface also has a major impact on bacterial adhesion [21]; however, the wettability of surfaces cannot last in long-term use. An active coating, which contains mesoporous materials or nanofibers, releases antibacterial agents such as metal ions, an antibiotic, free radicals, or nitrogen monoxide [7, 10, 13, 14, 15, 22, 23, 24, 25, 26, 27, 28, 29, 30]. Placing Ag ions on surfaces is the most widely studied technique as an antibacterial modality [24, 25, 29, 31, 32, 33, 34, 35, 36, 37, 38, 39, 40, 41]. An antibiotic [42], peptide [43, 44, 45], or organic compound like polycaprolactone or chitosan [28, 41, 46] have also been tested as antibacterial agents. Though these released antibacterial agents show adequate performance, controlling or maintaining these concentrations in body fluids is difficult. Unfortunately, the released antibacterial agents suppress osteointegration at the interfaces between implants with surrounding tissues. Antibacterial agents that do not obstruct osteointegration are preferable.

A multifunctional coating that can inhibit bacterial infection as well as maintain osteointegration was recently considered because of the crucial capacity for preventing revision of orthopedic implants [7, 13]. Multifunctional coatings are classified into a) those inhibiting bacterial adhesion via nontoxic compounds [14, 47, 48, 49], b) composites with controlled release of an antibacterial agent with an agent promoting osteoblast adhesion [50, 51, 52, 53], and c) those stimulating the release of an antibacterial agent, e.g., by UV irradiation or a magnetic field [54, 55]. The RGD peptide [14, 47, 48] can reduce bacterial adhesion whereas fibronectin can adhere to the surface covered by the RGD peptide. Nonetheless, the RGD peptide has no antibacterial effect (does not kill bacteria). A controlled release of an antibacterial agent such as Ag ions or gallium may reduce viability of bacteria while the activity of osteoblasts can be preserved [52, 53]. Balancing the release rate with a concentration of the agent is a challenge in long-term use. UV irradiation of a photocatalyst [54] or application of a magnetic field [55] may exert significant antibacterial effects, but they simultaneously affect human-cell viability. Light-activated antibacterial effects of nanofiber or nanofibrous membranes, which were made of organic molecules based on benzophenones or polyphenols, were reported [56, 57, 58]. When considering bonding coating onto the surface of metallic implants, multifunctional coatings based on plasma-spraying technology are beneficial because plasma-sprayed coatings have sufficient interfacial strength with metallic substrates. Matsuya et al. developed a composite coating containing a fluorescent complex of hydroxyapatite with a visible-light-responsive photocatalyst, and this composite coating has an antibacterial effect induced by visible-light irradiation [59, 60]. On the other hand, the ligand of the HAp complex was also cytotoxic. A visible-light-responsive plasma-sprayed coating, which can possess both antibacterial property and cytocompatibility, has not been developed to date.

Here we proposed a new biocompatible composite coating containing a fluorescent complex of HAp with gray titania, as shown in Fig. 1. HAp itself functioned as bacteria catchers and gray titania released antibacterial radicals by visible-light irradiation. HAp-amino acid fluorescent complexes were formed on the surface of the composite coating in order to increase light intensity to gray titania by fluorescence. Fabricating a fluorescent complex of HAp from biocompatible ligands such as amino acids can overcome the limitations seen in other studies [59, 60]. Therefore, the aim of this study is to reveal the enhancement mechanism of antibacterial properties of titania by HAp fluorescent complexes after light irradiation. A cytotoxicity assay involving osteoblasts and an antibacterial assay using *Escherichia coli* were conducted to clarify the performance of the proposed multifunctional coating. Bacteria on the surface of the coating, which are bound by the HAp complex, can be exposed to a higher concentration of radicals produced by a photocatalyst. Intensity of such interactions between bacteria and the surfaces of biomaterials has been investigated by atomic force microscopy (AFM)

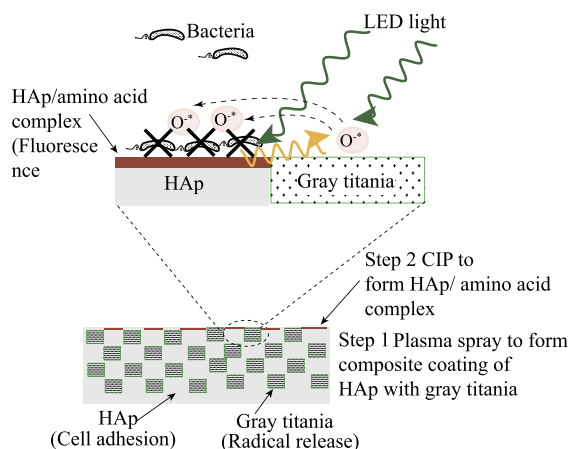


Fig. 1. The model of antibacterial properties of a composite photocatalyst with fluorescent HAp–amino acid complex as a coating under light irradiation.

[61, 62, 63, 64], which has uncovered the effects of wettability, surface roughness, or morphology on the bacterial adhesion behavior. Surface potential is also an important property affecting the adhesion behavior of bacteria on the surface of biomaterials [65, 66], and Kelvin force microscopy (KFM) can detect the changes in surface potential induced by light irradiation [67, 68]. The surface potential on the surface of HAp complexes under light irradiation was measured by KFM to elucidate its light-induced mechanism of enhancement of antibacterial properties.

## 2. Materials & methods

### 2.1. Fabrication of composite coating of HAp with gray titania

Ti-6Al-4V plates were machined to the dimensions of  $50 \times 10 \times 3$  mm. HAp powders (HAP-100, Taihei Chemical Co., Ltd., Japan) were sieved at approximately  $90 \mu\text{m}$  and were crushed by ball milling. The HAp powders were deposited on the Ti-6Al-4V plates by plasma spraying (model 9 MB, Seltzer Meteco under the following conditions: current of 500 A, controlling voltage of 68 V, particle feed rate of 15 g/min, and spraying distance of 140 mm). The average thickness of the HAp coating was approximately  $100 \mu\text{m}$ .  $\text{Ti}_2\text{O}_3$  powder (TIE02PB, Kojundo Chemicals, Japan) was sieved through  $90 \mu\text{m}$  mesh as well. The average particle size of  $\text{Ti}_2\text{O}_3$  was smaller than  $90 \mu\text{m}$ . The powder composed of 80 wt% HAp/20 wt%  $\text{Ti}_2\text{O}_3$  was mixed in a ball mill for 1 hour. Only photocatalyst coating exhibited insufficient antibacterial property due to the suppression of bacterial adhesion [69], and then we selected the ratio so that the surface of HAp particles can be partly covered by  $\text{Ti}_2\text{O}_3$  particles. Matsuya et al. reported that plasma-sprayed  $\text{Ti}_2\text{O}_3$  was transformed into Rutile ( $\text{TiO}_2$ ) with  $\text{Ti}_6\text{O}_{11}$ , which could produce oxygen radicals under visible-light irradiation [60]. They called the plasma-sprayed  $\text{Ti}_2\text{O}_3$  coating as gray titania coating [60], which is used in the present study.

### 2.2. Fabrication of the HAp complex with an amino acid by cold isostatic pressing (CIP)

Three amino acid ligands—phenylalanine (Phe), tryptophan (Trp), and tyrosine (Tyr) (Kishida Chemical Co., Ltd., Osaka, Japan)—were used for complexation with HAp. The three types of aromatic amino acids were selected due to their strong fluorescent property. Namely, 500 mg of an amino acid powder was placed on the surface of a plasma-sprayed HAp coating, and all the samples were sealed with plastic bags on a vacuum drawing machine. The sealed HAp coating was next dried in an incubator at  $40^\circ\text{C}$  for 24 h. Finally the sealed HAp coating bags were pressurized by CIP (Model P-500, Kobe Steel, Ltd., Japan) at maximum pressure 800 MPa and holding time 20 min [59].

### 2.3. Examination of fluorescence emitted by the HAp complex with amino acids

Fluorescent properties of HAp complexes with one of three amino acids were examined under ultraviolet irradiation with excitation wavelength of 315–400 nm (FPL27BLB, Sankyo Denki Co., Ltd.). The HAp amino acid complex coating was then immersed in distilled water for 7 days and 30 days in order to remove unreacted amino acid on the surface. HAp amino acid complex should be hardly soluble in water and then the remained fluorescence after the immersion can certify the existence of the complex. The wavelength of fluorescence was evaluated by luminescence microscopy (BZ-8100, Keyence Co., Ltd., Japan.), before and after 30-day immersion. Three types of excitation source,  $360 \pm 20$ ,  $470 \pm 20$ , and  $540 \pm 12.5$  nm with exposure time of 0.5 s were employed to observe blue ( $460 \pm 20$  nm), green ( $535 \pm 25$  nm), and red fluorescence ( $605 \pm 27.5$  nm).

### 2.4. Cytotoxicity assay

Mouse MC3T3-E1 osteoblasts (RIKEN Bioresource Center, Japan) were used to evaluate cytotoxicity of HAp fluorescent complexes with an amino acid. HAp fluorescent complexes with an amino acid coating were sterilized using an UV light. Plasma-sprayed HAp coating is used for metallic implants to enhance their osteoconductivity [1]. Osteoblast cells are used for observing cytocompatibility of HAp coating containing antibacterial agents in order to observe whether the osteoconductivity of HAp coating would be deteriorated by antibacterial agents [33, 70]. Osteoblasts were cultured in the high-glucose DMEM medium that was supplemented with 10% of fetal bovine serum (FBS), L-glutamine (WAKO, Osaka, Japan), and 1% of a Penicillin-Streptomycin solution (Sigma-Aldrich, Osaka, Japan), at 37 °C in an incubator (SANYO, MCO-18AC, 5% CO<sub>2</sub> with 100% humidity). A Trypsin-EDTA solution (0.05% w/v; WAKO, Osaka, Japan) served for cell detachment during subculturing. The MC3T3-E1 cells at  $8 \times 10^4$ /ml were also cultured on the surface of a fluorescent HAp-amino acid complex in 24-well plates for 24 h. The composition of the medium and cell density were determined by referring a previous study [71] for stable incubation. The adherent and proliferating cells were counted with Cell Counting Kit 8 (CCK8, DOTITE, Dojindo Laboratories, Japan) and their optical density was measured using a microplate reader with the filter wavelength of 450 nm. Values of optical density are proportional to the concentration of living cells containing in the medium and the significant decrease in the values of optical density indicates the toxicity of materials.

### 2.5. Evaluation of antibacterial properties of HAp fluorescent complexes with Gray titania

Antibacterial assays involving *E. coli* K12 were conducted to confirm the enhancing effects of HAp fluorescent complexes on antibacterial properties of gray titania under visible-light irradiation. We previously reported an effectiveness of HAp/8-Hydroxyquinoline complex as an enhancement agent of antibacterial property of gray titania [60]. However, 8-Hydroxyquinoline itself has cytotoxicity. *E. coli* was used in the antibacterial test in order to directly compare the enhancement effect by HAp fluorescent complex of the toxic ligand with the ones by the complexes without toxic ligands (amino acids). Several researches [50, 55] also used *E. coli* to discuss basic antibacterial property of their developed multifunctional coating. Three laser types of visible light, 425 nm (blue), 532 nm (green), and 630 nm (red), were used for irradiation at controlled irradiance of 50 mW/cm<sup>2</sup>. Both HAp/Gray titania coating and HAp complex/Gray titania coating were tested against bacterial *Escherichia coli* K12 (*E. coli*). The Luria-Bertani (LB) medium consisting of bacto tryptone (10 g/L), bacto yeast extract (5 g/L), NaCl (5 g/L), and deionized water, was sterilized in an autoclave at 120 °C, 1.2 ks (TOMY, SX-500). A suspension containing *E. coli* was cultured directly on an HAp coating in the LB medium. Turbidity was measured on a

spectrophotometer (Hitachi U-1100 at wavelength 600 nm). Because the initial values of OD fluctuated, OD values after specific hours were normalized to the one at 0 hour (immediately after light irradiation) to evaluate growth rate of *E. coli* [49, 60]. The *E. coli* suspension, following the incubation, was diluted 10<sup>7</sup>-fold. Next, 0.2 mL of the diluted suspension was grown on LB nutrient agar and incubated at 37 °C for 18 h. Colonies on the LB nutrient agar medium were counted in the pictures of the plates to determined colony forming units (CFUs). Percentage of control ( $C_{-}/L_{-}$ ) was calculated by the ratios of the CFUs for each case divided by the CFUs of control ( $C_{-}/L_{-}$ ). Lower values of percentage of control suggest decreased CFUs of bacteria, which exhibits the antibacterial effect by factors of laser irradiation or the existence of complex.

### 2.6. KFM analysis of the surface of HAp fluorescent complexes

KFM analyses of the surfaces of HAp or HAp-amino acid complexes were carried out to clarify the effects of ligands on surface potential during light irradiation. HAp plates made by CIP were employed for KFM to reduce the effect of surface roughness on this analysis. A fixed stand of LEDs was set in front of a scanning probe microscope, SPM-9700 (Shimadzu Science Co., Ltd.).

Two types of LED light, 425 nm (blue), and 532 nm (green) served for the irradiation at irradiance 50 mW/cm<sup>2</sup>. The measurement was conducted in a dark room at room temperature (25 °C). At first, KFM analyses before light irradiation were conducted in a region of 1000 × 1000 nm. Immediately after completion of the scanning by KFM cantilever, a LED lamp was turned on, and the same scan was repeated in the same region. Surface potential was calculated using the average value of the analyzed region, and the surface potentials before and after LED irradiation were designated as  $V_{off}$  and  $V_{on}$ , respectively. Changes in surface potential were calculated as  $V_{on} - V_{off}$ . Analytical conditions of KFM were as follows: laser potential at operating point of 0.2 V, frequency adjustment of 67 kHz, driving gain of 0.5, and I-gain of 700.0. The cantilever used in the KFM analysis was EFM-20 (Nanoworld Innovate Technology Product Corporation). The KFM analysis was performed in triplicate by moving to different positions for each type of HAp fluorescent complexes.

### 2.7. Statistical analysis

ANOVA and multiple comparison by Holm's method were applied to the results of the cytotoxicity assay, the antibacterial assay, and the KFM analysis. The significance level was set to  $p < 0.05$ . All statistical analyses were performed in the R3.4.2 software.

## 3. Results

### 3.1. Fluorescence wavelength for different ligands (amino acids)

The CIP process successfully fabricated HAp-amino acid complexes (Fig. 2), as in the case of a HAp-8-hydroxyquinoline complex [59]. Tris(8-hydroxyquinoline)aluminum (Alq3) is a typical fluorescent complex [23] and HAp with 8-hydroxyquinoline could form a fluorescent complex fabricated by mechanochemical method [72]. The result exhibited that Ca ion in HAp crystal with molecules of amino acid can also form a complex. Static compression of 800 MPa produced a coordination bond between Ca ions in the HAp crystal and an amino group in hydrophobic amino acids (Phe, Trp) or a hydrophilic amino acid (Tyr). The HAp-Phe and HAp-Tyr complexes manifested variation in wavelength from blue (Fig. 2A and C) whereas the HAp-Trp complex showed approximately yellow fluorescence (Fig. 2B). Changes in fluorescence from HAp-amino acid complexes were observed after water immersion. (Fig. 2). Fluorescence emitted by HAp-Trp and HAp-Phe complexes was certainly retained, thus confirming the stability of coordination bonds in the HAp-amino acid complexes in a liquid medium.

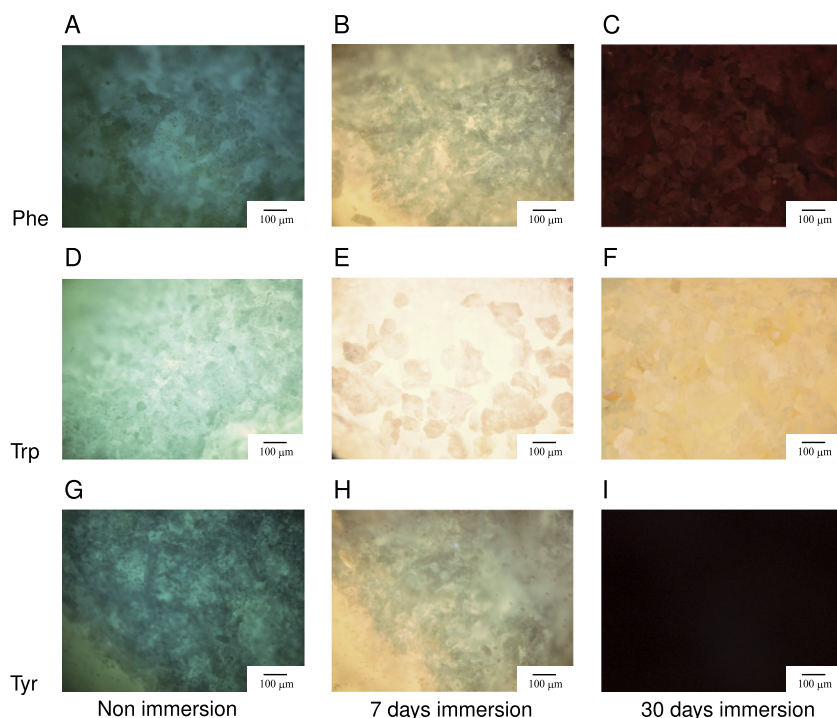


**Fig. 2.** Effects of types of ligand in HAp–amino acid complexes on fluorescence wavelength. (A–C) HAp–phenylalanine (Phe) complex. (D–F) HAp–tryptophan (Trp). (G–I) HAp–tyrosine (Tyr) complex. (A, D, G) Before immersion. (B, E, H) After 7-days immersion. (C, F, I) After 30-days immersion. All pictures are merged images of red, green, and blue fluorescent images. Exposure time in all images was 0.5 s.

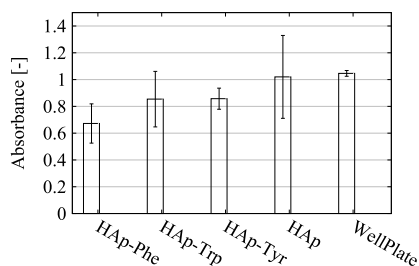


**Fig. 3.** Effects of ligands in HAp–amino acid complexes on toxicity toward MC3T3-E1 osteoblasts. Osteoblasts were directly cultured on the surface of every sample. Data are presented as the mean  $\pm$  standard deviation of triplicate samples ( $*p < 0.05$ ).

Fluorescence wavelength was red-shifted in the cases of HAp–Trp and HAp–Phe complexes due to the dissolution of unreacted amino-acids ligands (Fig. 2B, C, E, F), which was also reported by previous study [59]. We did not test a simulated body fluid in the assay to prevent precipitation of amorphous calcium phosphate, which blocked excitation light for the surface of HAp–amino acid complexes. A HAp fluorescent complex shows precipitation behavior equivalent to that of HAp itself [59].

### 3.2. Toxicity of HAp–amino acid complexes toward osteoblasts

Cytotoxicity of HAp–amino acid complexes was evaluated on MC3T3-E1 osteoblasts without light irradiation (Fig. 3). Although ANOVA detected a difference (F-value 2.39 [ $df = 14$ ],  $p = 0.02$ ), no significantly different pairs were detected by the multiple-comparison test (Holm's method). This result is due to the small deviation in plate wells and indicated that cytotoxicity of HAp–amino acid complexes is equivalent to that of HAp, which is considered enough to promote osteointegration.

### 3.3. Enhancing effects of HAp–amino acid complexes on antibacterial properties of gray titania

To confirm the enhancing effect of HAp–amino acid complexes on antibacterial properties,  $OD_{600}$  values were measured. Note that  $OD$  values were normalized to initial values [60]. Without complexes, radical generation by gray titania was not enough to reduce the growth rate (Fig. 4B). HAp–amino acid complexes significantly reduced the growth rates according to  $OD$  values even in the case without irradiation ( $L_-$ ), and red LED irradiation ( $L_{B+}$ ) was the most effective in reducing the growth rates ( $OD$  values) regardless of the type of ligand (Fig. 4C–E).

CFUs of *E. coli* were also assessed after 18 h cultivation to confirm the effects of both factors: the presence of complexes and types of irradiation. The best pair was a complex with red LED irradiation ( $C_+/L_{R+}$ ): the percentages of control ( $C_-/L_{R-}$ ) were  $26.9\% \pm 0.9\%$  (HAp–Phe complex),  $37.3\% \pm 5.6\%$  (HAp–Trp complex),  $19.0\% \pm 3.3\%$  (HAp–Tyr complex) (Fig. 5A–C). Such percentages of reduction were consistent with the ones reported for other types of multifunctional coating [50, 51, 52, 53, 54, 55], though the antibacterial property was not stronger than the one of conventional Ag ions and other materials [31, 32]. Two-factor ANOVA revealed that the factor of the presence of complexes had a significant effect, regardless of the type of LED irradiation (Fig. 5D–F). HAp complex cannot produce any antibacterial agent such as radicals by itself [60]. Therefore, the enhancing effect of HAp–amino acid complexes on antibacterial properties of gray titania was indispensable to achieve sufficiently strong antibacterial properties using a visible-light-sensitive photocatalyst.

### 3.4. The effect of light irradiation on the surface potential of HAp–amino acid complexes

Although only LED irradiation of gray titania produced free radicals as antibacterial agents, in some cases effects of LED ( $L_+$ ) on antibacterial property were not significant probably due to the reduced effect of HAp as cell catcher (Fig. 4). We then hypothesized that LED irradiation reduces cell adhesion performance of a HAp coating. To test

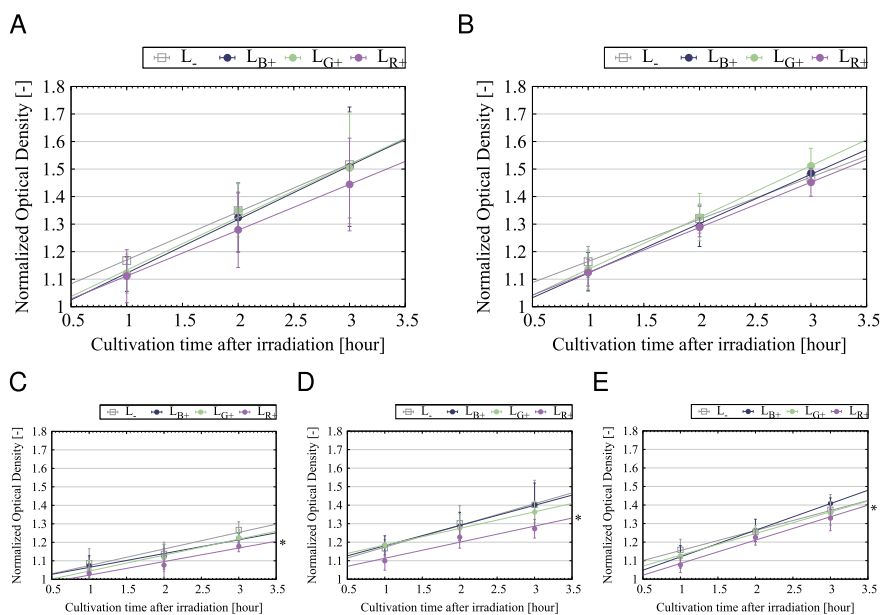


**Fig. 4.** Changes in OD values of an *E. coli* suspension under the influence of irradiation with LEDs. (A) HAp coating. (B) HAp-gray titania coating. (C) HAp-Phe complex/gray titania coating. (D) HAp-Trp complex/gray titania coating. (E) HAp-Tyr complex/gray titania coating. The types of LED irradiation  $L_-$ ,  $L_{B+}$ ,  $L_{G+}$ ,  $L_{R+}$  are no irradiation, blue LED irradiation, green LED irradiation, and red LED irradiation, respectively. Data are presented as the mean  $\pm$  standard deviation of triplicate samples ( $*p < 0.05$ ).

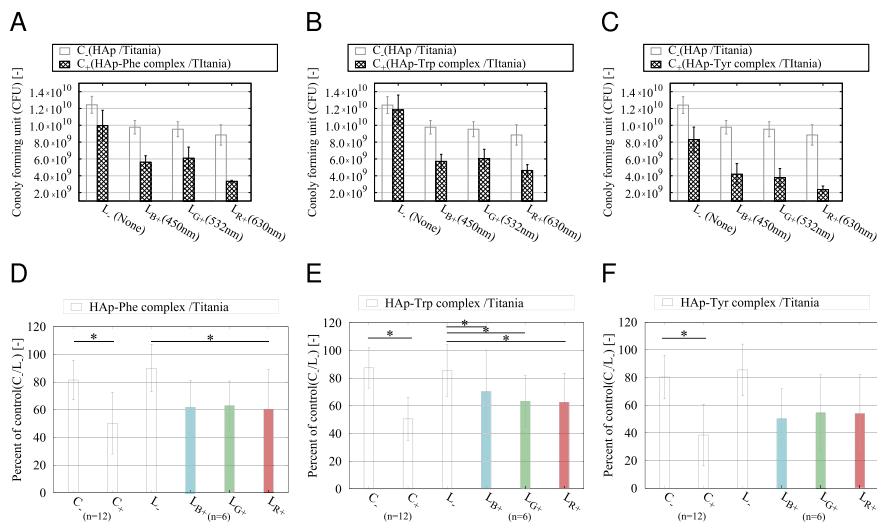


**Fig. 5.** Enhancing effects of HAP-amino acid complexes on antibacterial action of gray titania under irradiation with blue, green, or red LEDs. (A–C) Changes in CFUs. (D–F) Percentage of control ( $C_-/L_-$ ) for both factors: the presence of a complex and laser irradiation. Data are presented as the mean  $\pm$  standard deviation of triplicate samples ( $*p < 0.05$ ).

the hypothesis, surface potentials of HAP and HAP-amino acid complexes were examined by KFM. LED irradiation reduced the surface potential of HAP though that of HAP-amino acid complexes was not changed (Fig. 6A and B). The surface potentials of HAP-amino acid complexes were dependent on the type of ligand (Fig. 6C) and its order of magnitude seemed to negatively correlate with the percentage reduction in CFUs (Fig. 4A–C). LED irradiation significantly reduced the surface potential of HAP, and HAP-amino acid complexes inhibited such a reduction (Fig. 6D). Red LED was not suitable for the KFM analysis because it disturbed manipulation of the cantilever using the same wavelength. We also measured surface temperature by infrared (IR) thermography during LED irradiation both in the case of CFU evaluation and KFM, and no significant changes in temperature were observed. Consequently, HAP-amino acid complexes maintained the cell adhesion

performance of HAP during irradiation, which enhanced the antibacterial properties of gray titania induced by LED irradiation.

#### 4. Discussion

In this study, a CIP method for fabricating fluorescent complexes between HAP and an amino acid was successfully developed. The fluorescent complexes of HAP with one of amino acids were insoluble *in vitro* even after a long incubation (Fig. 2). The HAP/Phe complex after immersion showed red-shifted fluorescence, which exhibited the effect of CIP pressure on promoting molecular orientation of amino acid ligand and accompanying change in the fluorescent property. The red-shift fluorescence is attributed to an arrangement of Phe molecules onto the surface of HAP coating [73], and CIP process can exclusively promote

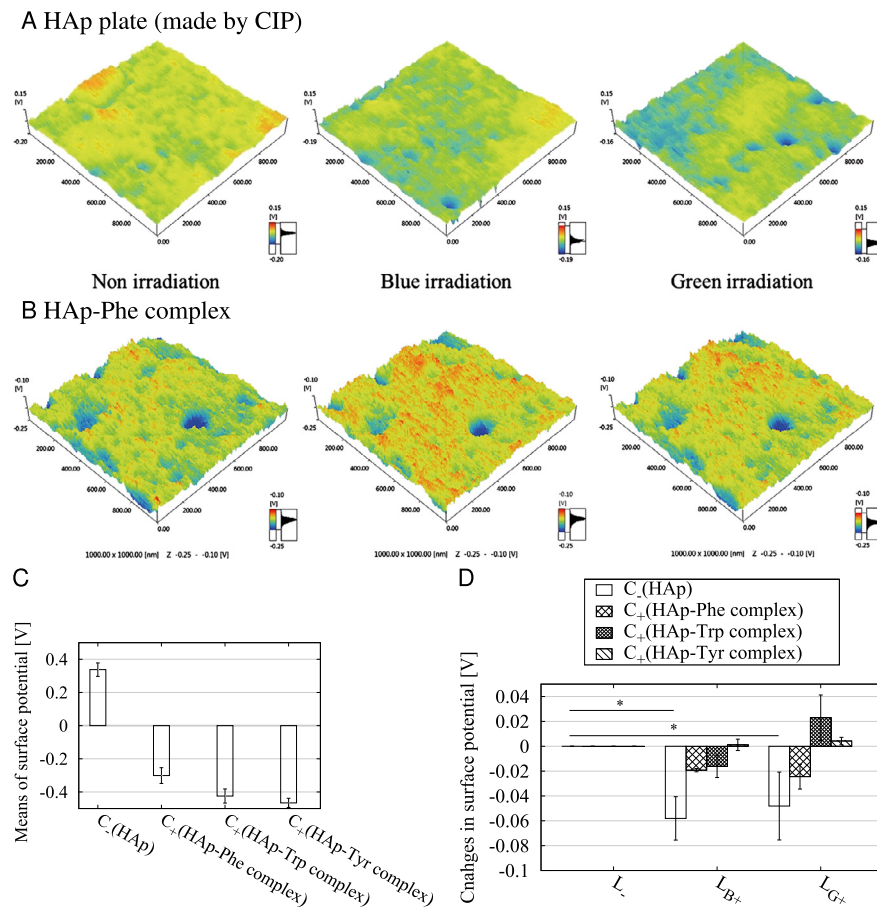


**Fig. 6.** The preserving effect of HAp-amino acid complex on the surface potential during irradiation with a LED. (A) Surface potential distributions of CIPed HAp. (B) Surface potential distributions of the CIPed HAp–Phe complex. (C) Surface potentials in the presence of different types of ligands. (D) Changes in surface potential during irradiation with LEDs. Types of LED irradiation  $L_-$ ,  $L_{B+}$ ,  $L_{G+}$  are no irradiation, blue LED irradiation, and green LED irradiation, respectively. Data are presented as the mean  $\pm$  standard deviation of triplicate samples (\* $p < 0.05$ ).

such an arrangement. Furthermore, the HAp–amino acid complexes were nontoxic to mouse osteoblastlike cells (Fig. 3): a favorable feature for multifunctional coating layers. The HAp–amino acid complexes successfully enhanced light-induced antibacterial properties of gray titania under visible light (Fig. 4). Although the strong fluorescence of the HAp–Trp complex (Fig. 2E–H) significantly amplified the antibacterial effect of gray titania (Fig. 5B and E), such an enhancing effect was usually significant regardless of the type of ligand (Fig. 5). We also observed changes in the surface potential of HAp coatings, which is one of critical factors in the regulation of cell adhesion behavior. HAp–amino acid complexes increased absolute values of surface potential and preserved the potential even under light irradiation (Fig. 6).

The enhancement mechanism is illustrated in Fig. 7. Band gap energy of HAp (5.0 eV [74]) is too high to be excited by visible light, and HAp can absorb only thermal energy of light, which can promote recombination of polarized pairs on its surface (Fig. 7A). A relation between light intensity and amplitude of an electric field of light is determined by the following equations (1), (2) of Beer's law [75]:

$$E(t) = E_0 \cos(\omega t) \quad (1)$$

$$|E_0| = \sqrt{\frac{I_{LED}}{\epsilon_0 n c}} \quad (2)$$

where  $\omega$  is angular frequency of light,  $I_{LED}$  is irradiance of light [ $\text{mW}/\text{cm}^2$ ], with permittivity of vacuum  $\epsilon_0 = 8.854 \times 10^{-12}$  F/m, refractive index  $n$ , and speed of light  $c = 2.998 \times 10^8$  m/s. Reflectance of light is then calculated via the equation (3),

$$R_{\perp} = \frac{(1-n)^2 - k^2}{(1-n)^2 + k^2} \quad (3)$$

where  $k$  is the extinction coefficient. Dielectric loss by the electric field is then calculated using the equation (4) [76]

$$\Delta E_{ele} = \frac{1}{2} \epsilon_0 \epsilon_1 \omega |E_0|^2 \tan \delta \quad (4)$$

where  $\epsilon_1 = n^2 - k^2$ ,  $\epsilon_2 = 2nk$ , and  $\tan \delta = \frac{\epsilon_2}{\epsilon_1}$ . If we consider recombination of polarized pairs by dielectric loss, then a reduction in electric potential can be calculated by means of the following equations (5), (6):

$$(1 - R_{\perp}) \Delta E_{ele} t_{ird} = \frac{1}{2} C (\Delta V)^2 \quad (5)$$

$$C = \frac{\epsilon_1 S}{d} \quad (6)$$

where  $t_{ird}$  is irradiation time (s),  $S$  is examined sample area 1 ( $\text{cm}^2$ ), and distance of recombination  $d$  is assumed to be 75 and 50 nm, respectively.  $n = 1.65$  and  $k = 0.000847$  were determined from experimental values by Bento et al. [77]. The calculated result of equations (2), (5) is in good agreement with the observed change in surface potential (Figs. 6C and 7B). Though the values of surface potential were so sensitive on surface morphology and insulation conditions of the samples [78], the magnitude of the changes were not matched in different samples (Figs. 6C and 7B). Weakened surface potential could detach bacteria from the surface, thereby leading to deterioration of antibacterial effectiveness. On the other hand, the amino acid complex has lower band gap energy [79, 80] and can emit fluorescence (Fig. 7A). Consequently, fluorescence can preserve the surface potential of the amino

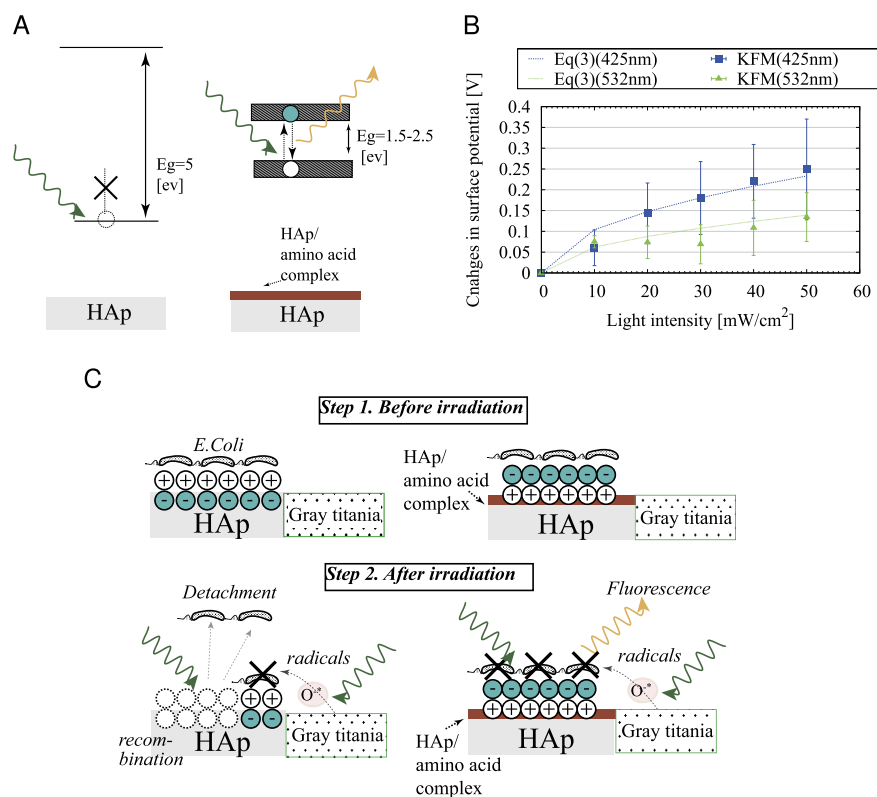


**Fig. 7.** Schematic illustration of the enhancing mechanism of the HAp–amino acid complex on antibacterial properties of titania via suppression of changes in surface potential. (A) A difference in optical band gap. (B) A calculated relation between light intensity and changes in voltage according to equations in the main text. (C) Different reactions during light irradiation; HAp manifested recombination of polarized pairs, and HAp complexes emitted fluorescence.

acid complex and then bacteria can strongly adhere to its surface. Such bound bacteria are subjected to higher concentrations of radicals and are effectively killed (Fig. 7C). Our finding first and foremost points out the importance of electric properties of HAp as a dielectric for antibacterial action.

A conventional multifunctional coating involving antibacterial agents has difficulty in regulating its antibacterial performance owing to uncontrollable solubility. The use of UV light can regulate the antibacterial action by adjusting irradiance, but UV itself also affects the surrounding tissues. The newly developed coating composed of HAp–amino acid complexes with titania can be activated by visible light, which leads to be a new type of multifunctional coating controllable *in vivo*. The newly developed coating made of HAp complexes with titania can be applied to enhance cell adhesion or detachment via appropriate selection of laser types and irradiance. Recently light-activated antibacterial effects of nanofiber or nanofibrous membranes, which were made of organic molecules based on benzophenones or polyphenols, were reported [56, 57, 58]. This study used inorganic material as photocatalyst. Combination of such organic photosensitizers with the proposed HAp complexes can provide different types of multifunctional coating.

The limitation is that the newly developed coating made of HAp complexes with titania was not optimized regarding its composition, and irradiation duration is still long when considering practical applications. Effects of irradiance and optimization of the mixing ratio of HAp with titania should be discussed further. The detailed observation of a mechanical interaction between the surface of HAp complexes and bacteria or mammalian cells can provide more quantitative data on interface mechanics, which should also be considered in further studies. Though radicals formed by light-irradiation to photocatalyst can commonly provide antibacterial effects on specific types of bacteria relating to dental or surgical implants [7, 12, 13, 16], further studies are also necessary to observe the variation in antibacterial property of proposed

HAp–amino acid complex with gray titania coating. HAp–amino acid complex can be retained in liquid environments, however, durability of antibacterial effects should be discussed further.

## 5. Conclusion

A CIP process successfully fabricated complexes of HAp with each of several amino acids as a fluorescent coating that is biocompatible and stable for use in human fluids *in vivo*. The HAp–amino acid complexes were retained in a liquid environment, and had no cytotoxicity to MC3T3-E1 osteoblast. Antibacterial testing against *E. coli* indicated a reduction in CFUs by an existing the HAp–amino acid complexes after visible-light irradiation. KFM measurement revealed that the surface potential of HAp–amino acid complex was maintained during light irradiation due to emission of fluorescence, which could suppress detachment of bacteria. The newly developed coating made of HAp complexes with titania can be applied to one of multifunctional coating.

## Declarations

### Author contribution statement

Sarita Morakul & Yuichi Otsuka: Conceived and designed the experiments; Performed the experiments; Analyzed and interpreted the data; Wrote the paper.

Kiyoshi Ohnuma: Conceived and designed the experiments; Analyzed and interpreted the data.

Motohiro Tagaya & Satoshi Motozuka: Analyzed and interpreted the data; Contributed reagents, materials, analysis tools or data.

Yukio Miyashita & Yoshiharu Mutoh: Conceived and designed the experiments; Contributed reagents, materials, analysis tools or data.

### Funding statement

This work was partly supported by JSPS KAKENHI [grant number 26870213] and by the Union Tool Foundation and MEXT Tri-Institutional Collaborative = Cooperative Educational Reform Project.

### Competing interest statement

The authors declare no conflict of interest.

### Additional information

The data is available by contacting the corresponding author.

### Acknowledgements

We thank Niigata Metallicon Co., Ltd., for producing the plasma-sprayed samples and Echigoseika Co., Ltd., for the use of a CIP machine. We also thank Ms. Afrina Khan Piya for supporting the analysis of fluorescence.

### References

- [1] R.B. Heimann, Thermal spraying of biomaterials, *Surf. Coat. Technol.* 201 (5) (2006) 2012–2019.
- [2] T.W. Bauer, J. Schils, The pathology of total joint arthroplasty ii. Mechanisms of implant failure, *Skelet. Radiol.* 28 (9) (1999) 483–497, cited by (since 1996): 161.
- [3] L. Sun, C.C. Berndt, K.A. Gross, A. Kucuk, Material fundamentals and clinical performance of plasma-sprayed hydroxyapatite coatings: a review, *J. Biomed. Mater. Res.* 58 (5) (2001) 570–592.
- [4] M. Røkkum, M. Brandt, K. Bye, K.R. Hetland, S. Waage, A. Reigstad, Polyethylene wear, osteolysis and acetabular loosening with an HA-coated hip prosthesis. A follow-up of 94 consecutive arthroplasties, *J. Bone Jt. Surg., Ser. B* 81 (4) (1999) 582–589.
- [5] O. Reikerås, R.B. Gunderson, Long-term results of ha coated threaded versus ha coated hemispheric press fit cups: 287 hips followed for 11 to 16 years, *Arch. Orthop. Trauma Surg.* 126 (2006) 503–508.
- [6] L. Palm, S.-A. Jacobsson, I. Ivarsson, Hydroxyapatite coating improves 8- to 10-year performance of the link {RS} cementless femoral stem, *J. Arthroplast.* 17 (2) (2002) 172–175.
- [7] S.B. Goodman, Z. Yao, M. Keeney, F. Yang, The future of biologic coatings for orthopaedic implants, *Biomaterials* 34 (13) (2013) 3174–3183.
- [8] E. Hansen, B. Zmistowski, J. Parvizi, Periprosthetic joint infection: what is on the horizon? *Int. J. Artif. Organs* 35 (10) (2012) 935–950.
- [9] H. Gupta, A. Garg, N. Bedi, Peri-implantitis: a risk factor in implant failure, *J. Clin. Diagn. Res.* 5 (1) (2011) 138–141.
- [10] B.R. Chrcanovic, T. Albrektsson, A. Wennerberg, Reasons for failures of oral implants, *J. Oral Rehabil.* 41 (6) (2014) 443–476.
- [11] K. Subramani, R. Jung, A. Molenberg, C. Hämmerle, Biofilm on dental implants: a review of the literature, *Int. J. Oral Maxillofac. Implants* 24 (4) (2009) 616–626.
- [12] M. Quirynen, M. De Soete, D. Van Steenberghe, Infectious risks for oral implants: a review of the literature, *Clin. Oral Implants Res.* 13 (1) (2002) 1–19.
- [13] J. Raphael, M. Holodny, S.B. Goodman, S.C. Heilshorn, Multifunctional coatings to simultaneously promote osseointegration and prevent infection of orthopaedic implants, *Biomaterials* 84 (2016) 301–314.
- [14] K. Bruehlhoff, J. Fiedler, M. Möller, J. Groll, R. Brenner, Surface coating strategies to prevent biofilm formation on implant surfaces, *Int. J. Artif. Organs* 33 (9) (2010) 646–653.
- [15] L. Zhao, P.K. Chu, Y. Zhang, Z. Wu, Antibacterial coatings on titanium implants, *J. Biomed. Mater. Res., Part B, Appl. Biomater.* 91B (1) (2009) 470–480.
- [16] B. Gottenbos, H.C. van der Mei, F. Klatter, D.W. Grijpma, J. Feijen, P. Nieuwenhuis, H.J. Busscher, Positively charged biomaterials exert antimicrobial effects on gram-negative bacilli in rats, *Biomaterials* 24 (16) (2003) 2707–2710.
- [17] M. Rahaman, B. Bal, W. Huang, Review: emerging developments in the use of bioactive glasses for treating infected prosthetic joints, *Mater. Sci. Eng. C* 41 (2014) 224–231.
- [18] L. Rimondini, S. Farè, E. Brambilla, A. Felloni, C. Consonni, F. Brossa, A. Carrassi, The effect of surface roughness on early in vivo plaque colonization on titanium, *J. Periodontol.* 68 (6) (1997) 556–562.
- [19] S.D. Puckett, E. Taylor, T. Raimondo, T.J. Webster, The relationship between the nanostructure of titanium surfaces and bacterial attachment, *Biomaterials* 31 (4) (2010) 706–713.
- [20] J. Podporska-Carroll, E. Panaitescu, B. Quilty, L. Wang, L. Menon, S.C. Pillai, Antimicrobial properties of highly efficient photocatalytic TiO<sub>2</sub> nanotubes, *Appl. Catal. B, Environ.* 176–177 (2015) 70–75.
- [21] D. Drake, J. Paul, J. Keller, Primary bacterial colonization of implant surfaces, *Int. J. Oral Maxillofac. Implants* 14 (2) (1999) 226–232.
- [22] R.-H. Dong, Y.-X. Jia, C.-C. Qin, L. Zhan, X. Yan, L. Cui, Y. Zhou, X. Jiang, Y.-Z. Long, In situ deposition of a personalized nanofibrous dressing via a handy electrospinning device for skin wound care, *Nanoscale* 8 (2016) 3482–3488.
- [23] S. Jiang, B.C. Ma, J. Reinholz, Q. Li, J. Wang, K.A.I. Zhang, K. Landfester, D. Crespy, Efficient nanofibrous membranes for antibacterial wound dressing and UV protection, *ACS Appl. Mater. Interfaces* 8 (44) (2016) 29915–29922.
- [24] V. Stabnikov, V. Ivanov, J. Chu, Construction biotechnology: a new area of biotechnological research and applications, *World J. Microbiol. Biotechnol.* 31 (9) (2015) 1303–1314.
- [25] J. Di, J. Price, X. Gu, X. Jiang, Y. Jing, Z. Gu, Drug delivery: ultrasound-triggered regulation of blood glucose levels using injectable nano-network (adv. healthcare mater. 6/2014), *Adv. Healthc. Mater.* 3 (6) (2014) 789.
- [26] E.Y. Teo, S.-Y. Ong, M.S.K. Chong, Z. Zhang, J. Lu, S. Mochhala, B. Ho, S.-H. Teoh, Polycaprolactone-based fused deposition modeled mesh for delivery of antibacterial agents to infected wounds, *Biomaterials* 32 (1) (2011) 279–287.
- [27] S. Jiang, L.-P. Lv, K. Landfester, D. Crespy, Nanocontainers in and onto nanofibers, *Acc. Chem. Res.* 49 (5) (2016) 816–823.
- [28] Y. Liu, W. Ma, W. Liu, C. Li, Y. Liu, X. Jiang, Z. Tang, Silver(i)glutathione biocoordination polymer hydrogel: effective antibacterial activity and improved cytocompatibility, *J. Mater. Chem.* 21 (2011) 19214–19218.
- [29] W. Chen, Y. Liu, H. Courtney, M. Bettenga, C. Agrawal, J. Bumgardner, J. Ong, In vitro anti-bacterial and biological properties of magnetron co-sputtered silver-containing hydroxyapatite coating, *Biomaterials* 27 (32) (2006) 5512–5517.
- [30] T. Shimazaki, H. Miyamoto, Y. Ando, I. Noda, Y. Yonekura, S. Kawano, M. Miyazaki, M. Mawatari, T. Hotokebuchi, In vivo antibacterial and silver-releasing properties of novel thermal sprayed silver-containing hydroxyapatite coating, *J. Biomed. Mater. Res., Part B, Appl. Biomater.* 92B (2) (2010) 386–389.
- [31] G.A. Fielding, M. Roy, A. Bandyopadhyay, S. Bose, Antibacterial and biological characteristics of silver containing and strontium doped plasma sprayed hydroxyapatite coatings, *Acta Biomater.* 8 (8) (2012) 3144–3152.
- [32] N.A. Trujillo, R.A. Oldinski, H. Ma, J.D. Bryers, J.D. Williams, K.C. Popat, Antibacterial effects of silver-doped hydroxyapatite thin films sputter deposited on titanium, *Mater. Sci. Eng. C* 32 (8) (2012) 2135–2144.
- [33] P.N. Lim, E.Y. Teo, B. Ho, B.Y. Tay, E.S. Thian, Effect of silver content on the antibacterial and bioactive properties of silver-substituted hydroxyapatite, *J. Biomed. Mater. Res., Part A* 101A (9) (2013) 2456–2464.
- [34] P.N. Lim, L. Chang, B.Y. Tay, V. Guneta, C. Choong, B. Ho, E.S. Thian, Proposed mechanism of antibacterial action of chemically modified apatite for reduced bone infection, *ACS Appl. Mater. Interfaces* 6 (19) (2014) 17082–17092.
- [35] A. Yanovska, A. Stanislavov, L. Sukhodub, V. Kuznetsov, V. Illiasenko, S. Danilchenko, L. Sukhodub, Silver-doped hydroxyapatite coatings formed on Ti-6Al-4V substrates and their characterization, *Mater. Sci. Eng. C* 36 (Supplement C) (2014) 215–220.
- [36] K. Herkendell, V. Shukla, A. Patel, K. Balani, Domination of volumetric toughening by silver nanoparticles over interfacial strengthening of carbon nanotubes in bactericidal hydroxyapatite biocomposite, *Mater. Sci. Eng. C* 34 (1) (2014) 455–467.
- [37] M.P. Sullivan, K.J. McHale, J. Parvizi, S. Mehta, Nanotechnology, *Bone Joint J.* 96-B (5) (2014) 569–573.
- [38] B. Tian, W. Chen, D. Yu, Y. Lei, Q. Ke, Y. Guo, Z. Zhu, Fabrication of silver nanoparticle-doped hydroxyapatite coatings with oriented block arrays for enhancing bactericidal effect and osteoinductivity, *J. Mech. Behav. Biomed. Mater.* 61 (Supplement C) (2016) 345–359.
- [39] Z.-C. Xiong, Z.-Y. Yang, Y.-J. Zhu, F.-F. Chen, Y.-G. Zhang, R.-L. Yang, Ultralong hydroxyapatite nanowires-based paper co-loaded with silver nanoparticles and antibiotic for long-term antibacterial benefit, *ACS Appl. Mater. Interfaces* 9 (27) (2017) 22212–22222.
- [40] H. Melero, C. Madrid, J. Fernández, J.M. Guilemany, Comparing two antibacterial treatments for bioceramic coatings at short culture times, *J. Therm. Spray Technol.* 23 (4) (2014) 684–691.
- [41] M. Kazemzadeh-Narbat, B.F. Lai, C. Ding, J.N. Kizhakkedathu, R.E. Hancock, R. Wang, Multilayered coating on titanium for controlled release of antimicrobial peptides for the prevention of implant-associated infections, *Biomaterials* 34 (24) (2013) 5969–5977.
- [42] Z.-B. Huang, X. Shi, J. Mao, S.-Q. Gong, Design of a hydroxyapatite-binding antimicrobial peptide with improved retention and antibacterial efficacy for oral pathogen control, *Sci. Rep.* 6 (2016).
- [43] J. Chen, Y. Zhu, Y. Song, L. Wang, J. Zhan, J. He, J. Zheng, C. Zhong, X. Shi, S. Liu, L. Ren, Y. Wang, Preparation of an antimicrobial surface by direct assembly of antimicrobial peptide with its surface binding activity, *J. Mater. Chem. B* 5 (2017) 2407–2415.

- [46] J. Shen, B. Jin, Y. Cheng Qi, Q. Ying Jiang, X. Feng Gao, Carboxylated chitosan/silver-hydroxyapatite hybrid microspheres with improved antibacterial activity and cytocompatibility, *Mater. Sci. Eng. C* 78 (Supplement C) (2017) 589–597.
- [47] L. Harris, S. Tosatti, M. Wieland, M. Textor, R. Richards, Staphylococcus aureus adhesion to titanium oxide surfaces coated with non-functionalized and peptide-functionalized poly(L-lysine)-grafted-poly(ethylene glycol) copolymers, *Biomaterials* 25 (18) (2004) 4135–4148.
- [48] F. Zhang, Z. Zhang, X. Zhu, E.-T. Kang, K.-G. Neoh, Silk-functionalized titanium surfaces for enhancing osteoblast functions and reducing bacterial adhesion, *Biomaterials* 29 (36) (2008) 4751–4759.
- [49] G. Bhardwaj, H. Yazici, T.J. Webster, Reducing bacteria and macrophage density on nanophase hydroxyapatite coated onto titanium surfaces without releasing pharmaceutical agents, *Nanoscale* 7 (2015) 8416–8427.
- [50] X. Chatzistavrou, J. Fenno, D. Faulk, S. Badyal, T. Kasuga, A. Boccaccini, P. Papagerakis, Fabrication and characterization of bioactive and antibacterial composites for dental applications, *Acta Biomater.* 10 (8) (2014) 3723–3732.
- [51] P.N. Lim, Z. Wang, L. Chang, T. Konishi, C. Choong, B. Ho, E.S. Thian, A multi-material coating containing chemically-modified apatites for combined enhanced bioactivity and reduced infection via a drop-on-demand micro-dispensing technique, *J. Mater. Sci., Mater. Med.* 28 (1) (2016) 3.
- [52] M. Kurtjak, M. Vukomanović, L. Kramer, D. Suvorov, Biocompatible nanogallium/hydroxyapatite nanocomposite with antimicrobial activity, *J. Mater. Sci., Mater. Med.* 27 (11) (2016) 170.
- [53] A. Cochis, B. Azzimonti, C.D. Valle, E.D. Giglio, N. Bloise, L. Visai, S. Cometa, L. Rimondini, R. Chiesa, The effect of silver or gallium doped titanium against the multidrug resistant acinetobacter baumannii, *Biomaterials* 80 (Supplement C) (2016) 80–95.
- [54] K. Welch, Y. Cai, H. Engqvist, M. Strømme, Dental adhesives with bioactive and on-demand bactericidal properties, *Dent. Mater.* 26 (5) (2010) 491–499.
- [55] I. Bajpai, K. Balani, B. Basu, Synergistic effect of static magnetic field and HA-Fe<sub>3</sub>O<sub>4</sub> magnetic composites on viability of *S. aureus* and *E. coli* bacteria, *J. Biomed. Mater. Res., Part B, Appl. Biomater.* 102 (3) (2014) 524–532.
- [56] S. Jiang, B.C. Ma, W. Huang, A. Kaltbeitzel, G. Kizisavas, D. Crespy, K.A.I. Zhang, K. Landfester, Visible light active nanofibrous membrane for antibacterial wound dressing, *Nanoscale Horiz.* 3 (2018) 439–446.
- [57] M. Arenbergerova, P. Arenberger, M. Bednar, P. Kubat, J. Mosinger, Light-activated nanofibre textiles exert antibacterial effects in the setting of chronic wound healing, *Exp. Dermatol.* 21 (8) (2012) 619–624.
- [58] Y. Si, Z. Zhang, W. Wu, Q. Fu, K. Huang, N. Nitin, B. Ding, G. Sun, Daylight-driven rechargeable antibacterial and antiviral nanofibrous membranes for bioprotective applications, *Sci. Adv.* 4 (3) (2018) eaar5931.
- [59] T. Matsuya, Y. Otsuka, M. Tagaya, S. Motozuka, K. Ohnuma, Y. Mutoh, Formation of stacked luminescent complex of 8-hydroxyquinoline molecules on hydroxyapatite coating by using cold isostatic pressing, *Mater. Sci. Eng. C* 58 (2016) 127–132.
- [60] T. Matsuya, S. Morakul, Y. Otsuka, K. Ohnuma, M. Tagaya, S. Motozuka, Y. Miyashita, Y. Mutoh, Visible light-induced antibacterial effects of the luminescent complex of hydroxyapatite and 8-hydroxyquinoline with gray titania coating, *Appl. Surf. Sci.* 448 (2018) 529–538.
- [61] O.H. Willemsen, M.M. Snel, K.O. van der Werf, B.G. de Grooth, J. Greve, P. Hinterdorfer, H.J. Gruber, H. Schindler, Y. van Kooyk, C.G. Figdor, Simultaneous height and adhesion imaging of antibody-antigen interactions by atomic force microscopy, *Biophys. J.* 75 (5) (1998) 2220–2228.
- [62] Y.-L. Ong, A. Razatos, G. Georgiou, M.M. Sharma, Adhesion forces between *E. coli* bacteria and biomaterial surfaces, *Langmuir* 15 (8) (1999) 2719–2725.
- [63] C. Canale, A. Petrelli, M. Salerno, A. Diaspro, S. Dante, A new quantitative experimental approach to investigate single cell adhesion on multifunctional substrates, *Biosens. Bioelectron.* 48 (Supplement C) (2013) 172–179.
- [64] F. Alam, K. Balani, Adhesion force of staphylococcus aureus on various biomaterial surfaces, *J. Mech. Behav. Biomed. Mater.* 65 (2017) 872–880.
- [65] I. Lee, E. Chung, H. Kweon, S. Yiaccomi, C. Tsouris, Scanning surface potential microscopy of spore adhesion on surfaces, *Colloids Surf. B, Biointerfaces* 92 (2012) 271–276.
- [66] S. Sakata, Y. Inoue, K. Ishihara, Precise control of surface electrostatic forces on polymer brush layers with opposite charges for resistance to protein adsorption, *Biomaterials* 105 (2016) 102–108.
- [67] G.H. Enevoldsen, T. Glatzel, M.C. Christensen, J.V. Lauritsen, F. Besenbacher, Atomic scale Kelvin probe force microscopy studies of the surface potential variations on the TiO<sub>2</sub>(110) surface, *Phys. Rev. Lett.* 100 (2008) 236104.
- [68] L. Gross, F. Mohn, P. Liljeroth, J. Repp, F. Giessibl, G. Meyer, Measuring the charge state of an atom with noncontact atomic force microscopy, *Science* 324 (5933) (2009) 1428–1431.
- [69] M.R. Elahifard, S. Rahimnejad, S. Haghghi, M.R. Gholami, Apatite-coated Ag/AgBr/TiO<sub>2</sub> visible-light photocatalyst for destruction of bacteria, *J. Am. Chem. Soc.* 129 (31) (2007) 9552–9553.
- [70] D. Ke, A. Vu, A. Bandyopadhyay, S. Bose, Compositionally graded doped hydroxyapatite coating on titanium using laser and plasma spray deposition for bone implants, *Acta Biomater.* 84 (2019) 414–423.
- [71] C. Fu, H. Bai, Q. Hu, T. Gao, Y. Bai, Enhanced proliferation and osteogenic differentiation of MC3T3-E1 pre-osteoblasts on graphene oxide-impregnated PLGA-gelatin nanocomposite fibrous membranes, *RSC Adv.* 7 (15) (2017) 8886–8897.
- [72] M. Tagaya, S. Motozuka, T. Kobayashi, T. Ikoma, J. Tanaka, Mechanochemical preparation of 8-hydroxyquinoline/hydroxyapatite hybrid nanocrystals and their photofunctional interfaces, *Ind. Eng. Chem. Res.* 51 (34) (2012) 11294–11300.
- [73] S. Morakul, Y. Otsuka, A. Nararya, M. Tagaya, S. Motozuka, K. Ohnuma, Y. Miyashita, Y. Mutoh, Effects of compression on orientation of ligands in fluorescent complexes between hydroxyapatite with amino acids and their optical properties, *J. Mech. Behav. Biomed. Mater.* 88 (2018) 406–414.
- [74] V. Bystrov, C. Piccirillo, D. Tobaldi, P. Castro, J. Coutinho, S. Kopyl, R. Pullar, Oxygen vacancies, the optical band gap ( $E_g$ ) and photocatalysis of hydroxyapatite: comparing modelling with measured data, *Appl. Catal. B, Environ.* 196 (2016) 100–107.
- [75] K. Ema, *Basic of Photophysics*, Asakura Publishing Co. Ltd., 2001.
- [76] C. Hamaguchi, N. Mori, *Electronic Properties of Solids*, Asakura Publishing Co. Ltd., 2014.
- [77] A. Bento, D. Almond, S. Brown, I. Turner, Thermal and optical characterization of the calcium phosphate biomaterial hydroxyapatite, *J. Appl. Phys.* 79 (9) (1996) 6848–6852.
- [78] T. Ezaki, A. Matsutani, K. Nishioka, D. Shoji, M. Sato, T. Okamoto, T. Isobe, A. Nakajima, S. Matsushita, Surface potential on gold nanodisc arrays fabricated on silicon under light irradiation, *Surf. Sci.* 672–673 (2018) 62–67.
- [79] P.S. Subramanian, E. Suresh, P. Dastidar, S. Waghmode, D. Srinivas, Conformational isomerism and weak molecular and magnetic interactions in ternary copper(II) complexes of [Cu(AA)]ClO<sub>4</sub>·nH<sub>2</sub>O, where AA = l-phenylalanine and l-histidine, l = 1, 10-phenanthroline and 2, 2-bipyridine, and n = 1 or 1.5: synthesis, single-crystal x-ray structures, and magnetic resonance investigations, *Inorg. Chem.* 40 (17) (2001).
- [80] M.-M. Duvenhage, M. Ntwaeaborwa, H.G. Visser, P.J. Swarts, J.C. Swarts, H.C. Swart, Determination of the optical band gap of Alq<sub>3</sub> and its derivatives for the use in two-layer OLEDs, *Opt. Mater.* 42 (2015) 193–198.